Photo-assisted Flow Battery Charging
College of Engineering Honors Capstone Project

Wes Fermanich[1]
Prof. David Kwabi[2]
[1]Department of Materials Science and Engineering
[2]Department of Mechanical Engineering
University of Michigan

Abstract
The rapid increase in renewable energy in our electrical grid has driven the need for energy storage systems to mitigate the effects of intermittent renewable sources. The coupling of renewable energy sources such as photovoltaics with batteries can lead to space and efficiency losses due to the interconnection of the two systems through wiring. A potential method for conjoining solar energy generation with energy storage is through a technology known as solar flow batteries. These batteries utilize dye-sensitized solar cells to aid in the charging process of the battery. In this project a methodology for fabricating working photoanodes for usage in a solar flow battery is laid out in detail. Photoanodes are fabricated and tested through polarization testing and SEM imaging to determine the electrical and surface properties respectively. Photoanode samples with a maximum power output of ~0.1 mW/cm^2 are shown but also demonstrate highly unideal solar cell performance through fill factor values ranging from 30-40%. Further work is then laid out on avenues to explore in detail to address the low performance values of photoanodes fabricated through the process detailed.

Introduction

The reality of climate change is driving the transition of our electricity grid away from fossil fuel-based power and towards a grid that is made up of increasingly high amounts of renewable energy. Renewable energy sources such as wind and solar suffer from intermittency issues due to their dependence on weather-related events. To be able to utilize these resources when demand is highest, coupling these systems with battery storage allows for greater flexibility of use. However, the coupling of these systems can suffer losses due to the necessary connections between the two systems. A potential space and energy-efficient solution is to directly integrate solar energy conversion and energy storage into one system as opposed to coupling separate PV and battery systems.[1] This unique pairing is done through the usage of dye-sensitized solar cells (DSCs) which are a unique kind of solar cell that uses a dye molecule to collect sunlight and then react with nearby electrolyte to regenerate. Integrating solar charging into redox flow batteries is a promising solution as the solar conversion component utilizes the same liquid electrolyte as the energy storage component.[2] The combined structure of a DSC and a redox flow battery is known as a solar flow battery of which a structure can be seen in Figure **1**, below.
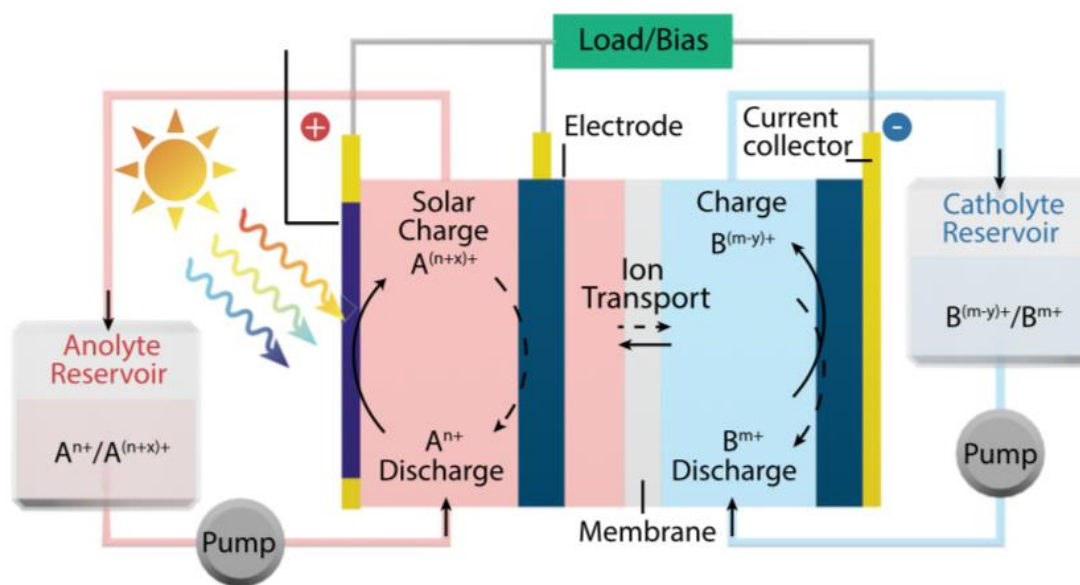
Figure 1. Schematic of a solar flow battery structure.[3]

Redox Flow Batteries

The basis for a solar flow battery is a redox flow battery, a type of electrochemical storage that is similar in structure to fuel cell. Redox flow batteries are made up of a few main components: an anode and cathode, anolyte and catholyte for driving oxidation reduction reactions at the electrodes, an ion-selective membrane, and pumps to drive the electrolyte through the respective halves of the cells. Though Figure **1** is of a solar flow battery, all the listed components are also visible in the figure. When a flow battery is undergoing a charging process the positive electrode or anode drives an oxidation reaction while the negative electrode or cathode drives a reduction

reaction with the surrounding electrolyte. During a discharging reaction the respective reaction type takes place at the opposite electrode.

Redox flow batteries on their own are a promising method for utility-scale energy storage due to their unique property of decoupling power and energy.[4] The amount of energy that can be stored is proportional to the size of the electrolyte tank or volume. As more electrolyte is circulated through the system, more energy can be stored. The power of the battery is proportional to the flow rate of said electrolyte as well as the design of the electrodes on either side of the cell. This scalability of the energy and power in tandem with the low volumetric energy density of redox flow batteries makes them a prime candidate for large-scale energy storage solutions such as for grid resiliency or load-shifting operations.[5]

Dye-sensitized Solar Cells (DSCs)
The structure of a DSC is made up of three main components: the transparent conductive oxide glass, the titanium dioxide (TiO_2) semiconducting thin film, and the light absorbing dye molecule. These three components make up the main structure which in the context of a solar flow battery will be referred to as the photoanode. When struck by sunlight the dye molecule becomes excited and elevates an electron into the conduction band of the TiO_2 thin film, allowing the electron to be conducted through the structure of the film and onto the transparent conductive oxide where it is syphoned to the external load. The thin film is made up of TiO_2 nanoparticles that form a interconnected, mesoporous structure that allows for the electrolyte to permeate through the structure. This mesoporous structure gives the photoanode a very high surface area for reactions to take place upon and for the dye molecules to attach to. The dyes used can be a range of molecules ranging from fruit juices to highly refined molecules.[6] For this study, a dye known as the Z-907 dye is used due to its high lifecycle stability and wide light absorbance spectrum.

Solar Flow Batteries
When photoanodes are integrated into a flow battery system they become known as a solar flow battery which functions largely the same as a regular flow battery but with an added solar charging component. When the photoanode is exposed to sunlight it acts to reduce the voltage necessary to drive the charging reaction in the flow battery through its photogeneration of energy. This reduction in charging voltage leads to a reduction in energy needed to charge the battery leading to the photo-assisted charging effect that this project is focused around.

Problems Addressed
The minimum goal of this research project was to establish a methodology for producing and testing the photoanodes to be utilized in solar flow batteries. Though this is a process that has been relatively well documented in literature, doing so utilizing the resources available and understanding the idiosyncrasies of producing these samples.[7] This involves developing a detailed set of methods for every step of the photoanode so that a person unfamiliar with the project

would be able to follow the process with little to no outside help aside from equipment trainings. This methodology would serve as the baseline for further research into the performance of the photoanodes. In this case, identification of speicifc areas for future work would be identified to improve the performance of the photoanodes.

The higher level or reach goal of this project would be to develop photoanodes that achieve a high level of current generation, ideally above 1 mA/cm^2, a level that has been demonstrated in literature as a strong baseline for solar flow battery performance. This was a listed as a stretch goal for this project due to the level of refinement and iteration required to develop a process that is consistent in producing high performance photoanodes.

Methods
Being a project with no previous experimental work at Michigan, this project involved developing the experimental process purely through literature review and communication with faculty and staff. Much of the process for photoanode development was based off the work done Wu et al. (2015) in developing an aqueous lithium-iodine solar flow battery.[8]

Photoanode Fabrication
As mentioned previously, the three main components of a photoanode are the conductive oxide glass, TiO$_2$ paste, and a dye molecule for light absorption. Fluorine-doped tin oxide (FTO) glass (Sigma-Aldrich) was used as the conductive substrate for building the photoanodes. Depending on the test, FTO samples were cut anywhere from 10mm x 30mm up to 40mm x 80mm. Using a multimeter on the resistance setting, the conductive side of the FTO was identified. Prior to being used in fabrication, FTO samples were either washed under a direct stream of ethanol or sonicated while submerged in ethanol for five minutes and then dried under a constant stream of pressurized air. This cleaning process serves to eliminate any contaminates that may have gotten onto the surface of the FTO.

TiO$_2$ paste was then mixed using four constituents: titanium (IV) oxide nanopowder (21 nm, Sigma-Aldrich), deionized water, acetylacetone (Sigma-Aldrich), and Triton X-100 (Fisher Scientific). The TiO$_2$ nanopowder serves as the basis for the paste with a primary particle size of 21 nm, aimed at creating a mesoporous structure with a high surface area for contact with the electrolyte. Deionized water acts as the main solvent for the paste by decreasing the viscosity of the paste. Acetylacetone is used as a dispersive agent to impede TiO$_2$ particle agglomeration. Triton X-100 functions as a surfactant to facilitate particle dispersion over the FTO substrate. TiO$_2$ nanopowder was added to a mixing cup, followed by deionized water, acetylacetone, and Triton X-100 with mixing in a Flack Tek dual axis speed mixer at 2000 rpm for 60 seconds between every addition and for 2 minutes after the final additions. The ratios of the constituents used were varied due to issues with cracking of the pastes after air drying due to the rapid drying speed. The cracked samples can be seen in Figure **2** below. The acetylacetone ratio was lowered due to its rapid

evaporation rate contributing to the rapid drying speed. The final ratios of constituents were 2000 mg TiO_2 nanopowder: 2900 μL deionized water: 110 μL acetylacetone: 110 μL Triton X-100.


Figure 2. Photoanodes produced prior to reduction in the acetylacetone ratio reduction.

Titania paste was applied to the conductive side of the FTO glass using the doctor blade method. Using a 1.0 mil tape (W.W. Grainger) as a mask to apply the paste in a lane with three millimeters of masked area on either side of the lane. The doctor blade height was adjusted to allow the blade to pass over the tape mask with as little clearance as possible. After being doctor bladed, the samples were air dried before the tape masks were removed and then the samples were placed into a furnace to at 450ºC to anneal for 30 minutes before being cooled completely.

Photoanodes were sensitized in a solution of 0.3 mM Z-907 dye (Sigma-Aldrich) and 30 mM Chenodeoxycholic acid (Sigma-Aldrich) in ethanol. Once removed from the solution, samples were air dried inside a fume hood before used in testing or set aside until tested. Photoanode samples were sensitized for varying amounts of time to test the effects of sensitization time on current and power production.

Polarization Testing
Photoanode samples were tested using a custom set up for electrochemical testing as shown below in **Figure 3**. The custom cell was designed in conjunction with one of graduate students in the Kwabi Group. The testing was conducted using an Oriel LCS-100 solar simulator at roughly 2 cm from the lamp end and in an aqueous electrolyte solution of 2.0 M lithium iodide (Sigma-Aldrich), 0.05 M iodine, and 1.0 M potassium chloride (Sigma-Aldrich).
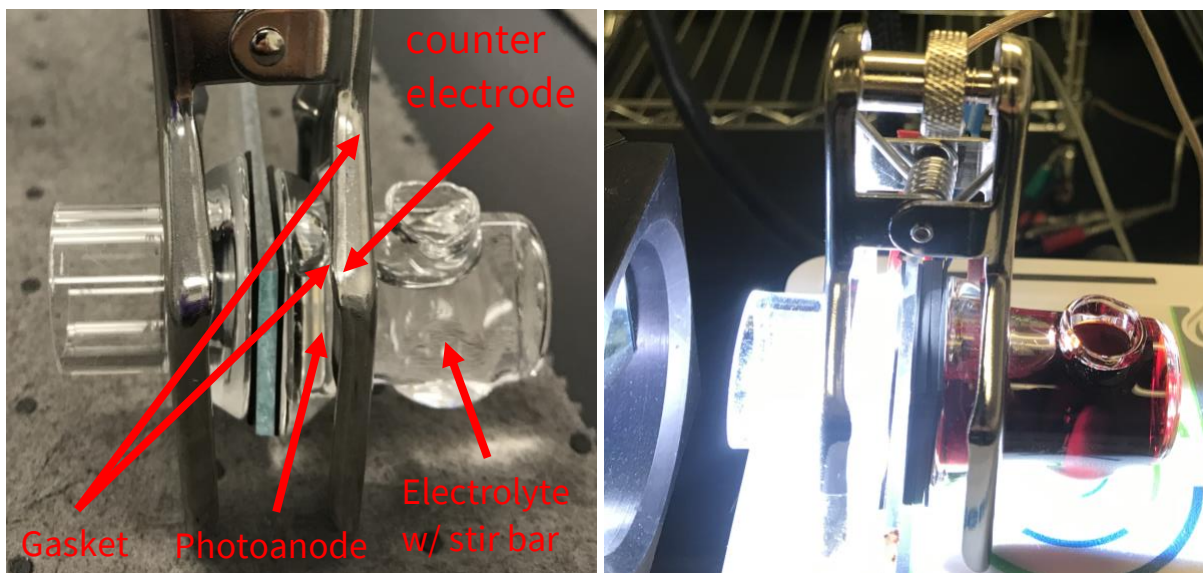
Figure 3. Photoanode electrochemical testing set up without electrolyte and light source (left) and filled with electrolyte under illumination (right).

Polarization tests were carried out using a porous graphite electrode attached to a gold wire as the counter and reference electrodes with the photoanode acting as the working electrode. Polarization tests were conducted at a scan rate of 50 mV/s with one test under illumination and another test taking place with the shutter of the light source closed. Polarization tests show the response of the current through an electrochemical setup as a voltage is cycled from low to high and back down, showing the current generation of the photoanode under the light source. All tests were using a Gamry potentiostat and Gamry software.

Results

Six different samples were tested using the same conditions to evaluate the effects of sensitization time on the power generation of the photoanodes as well as to establish a baseline for performance levels. The six samples can be seen below in **Figure 4**. All samples have the same surface area, roughly 2.5 cm^2, aside from sample S2 which has an active surface area of about 3.1 cm^2. To account for this, another sample value called "S2 norm" will indicate the S2 sample's value normalized to use the same surface area for all samples.
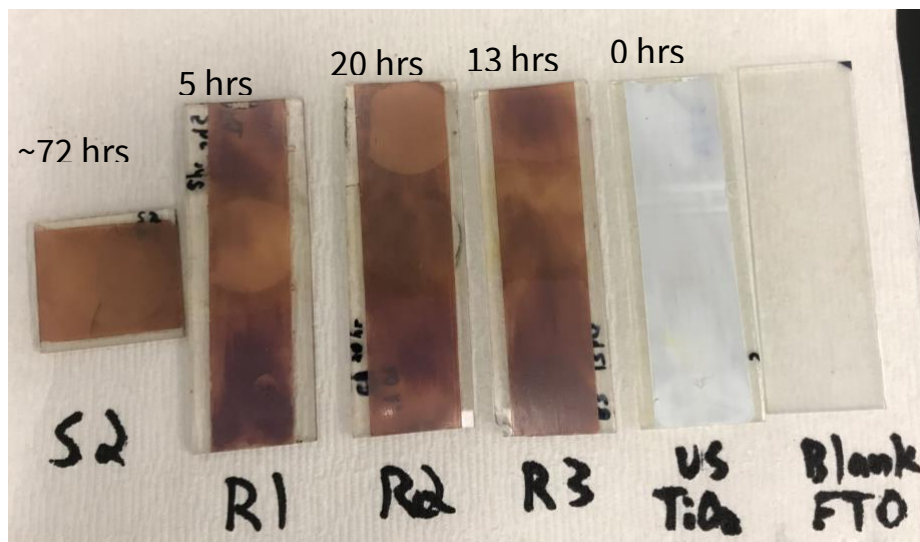
Figure 4. All samples tested with corresponding names and sensitization times

Polarization tests were carried out for all six samples under illumination and without illumination. It was determined that the unsensitized and uncoated samples showed no effect under the solar simulator when compared to their performance without the solar simulator. Therefore, the results for current and power generation will not contain the unsensitized and uncoated samples. The results for current and power generation are plotted on a positive scale for clarity in **Figure 5** below.
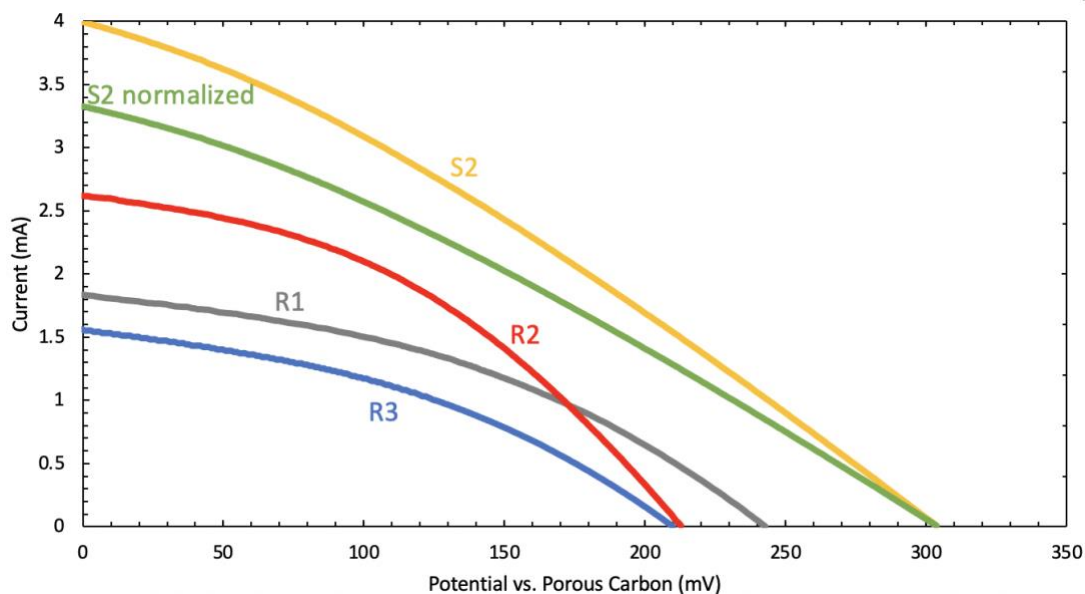

Figure 5. Polarization curves with bounds restricted to the region of photocurrent generation

The internal power loses in the cell can be characterized by taking the inverse positive slopes of the polarization curves from where they cross the potential axis. This value is known as the series resistance (Rs) in the cell and takes into account any losses that occur due to metal contacts or

from the bulk substrate.[9] High R_S values lead to reductions in the peak power production but do not affect the short circuit current (I_{SC}), where voltage is zero, or the open circuit potential (E_{OC}), where current is equal to zero.

Using the polarization curves, power versus potential curves were calculated and are shown below in **Figure 6**.
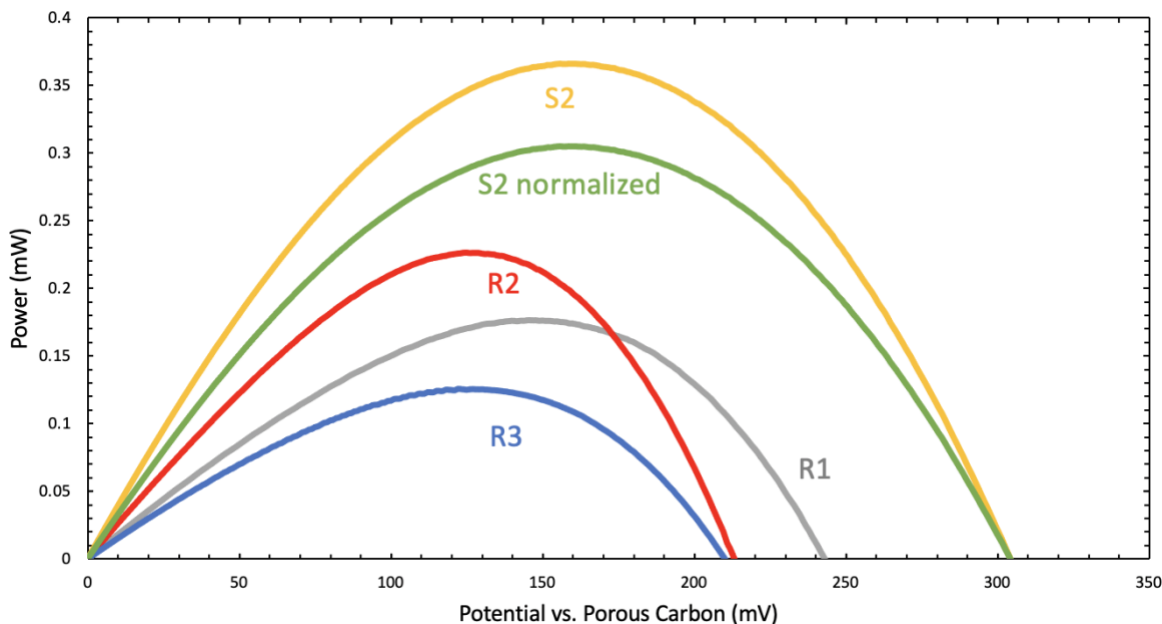
Figure 6. Power curves using the same potential range as the polarization curves

These two graphs can be used to characterize how close to an ideal solar cell these photoanodes are through their fill factor values which is a measure of their actual power production as a percentage of their theoretical power production as determined from their short circuit currents and open circuit potentials. Values for fill factors, series resistances, and other key metrics can be found in **Table 1** below.

Table 1. Performance parameters for all photoanode samples along with sensitization times

Sample	Sensitization Time (hrs)	E_{OC} (mV)	I_{SC} (mA)	P_{Max} Theoretical (mW)	P_{Max} (mW)	Fill Factor	R_S (Ω)
R1	5	243	1.83	0.445	0.176	39.6%	32.4
R2	20	213	2.62	0.558	0.226	40.5%	29.0
R3	13	210	1.56	0.328	0.126	38.5%	35.8
S2	~72	304	3.99	1.21	0.366	30.2%	47.4
S2 norm	~72	304	3.32	1.01	0.305	30.2%	-

The results gathered from all polarization tests are summarized together in **Table 1** showing the varying ranges for each parameter amongst the set of tested samples. To investigate a possible reason for these inconsistent and low performance metrics, SEM images were taken of unsensitized photoanode sample prior to and after being annealed and can be seen below in **Figure 7**.
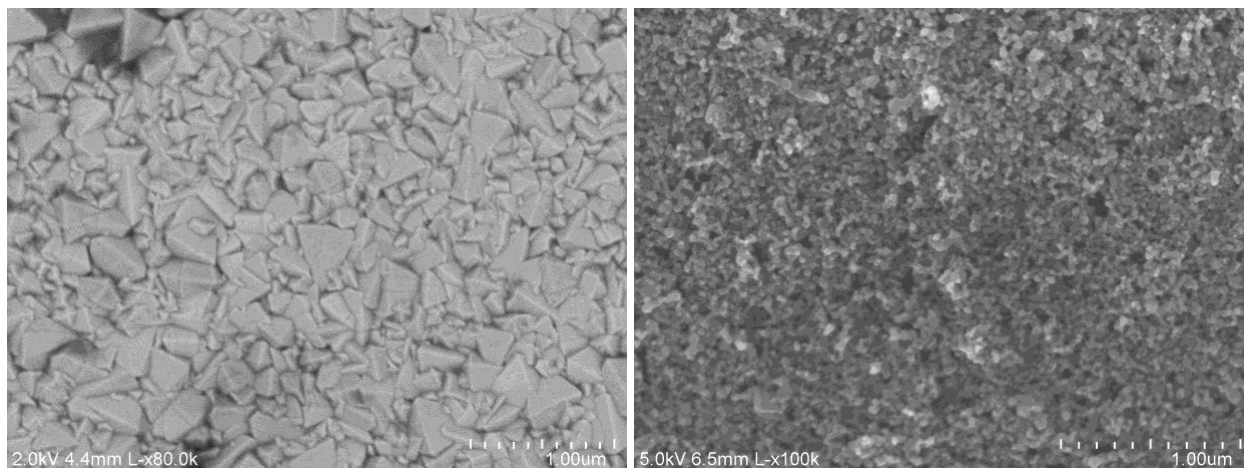
Figure 7. SEM images on the 1-micron scale of pre-annealing (left) and post-annealing (right) unsensitized photoanode samples

As evident above, significant changes are obvious in the surface topology of the photoanode samples as a result of the annealing process. The annealing process clearly increases the surface area of the photoanode, allowing for more area for recombination reactions to take place.

Discussion

Referring to **Table 1**, the most important results is that there is clear photogeneration taking place when the sample are exposed to the solar lamp. Regardless of the sensitization time, current is being generated which does not occur in the unsensitized or blank FTO samples. This means that the photoanode production process as detailed above is valid a proof of concept for producing light-active photoanodes. This means that the minimum goals for this project have been achieved.

The fill factors of the cells are the next most notable metric with all of them being at or below 40%. This is nearly half of the value of typical DSCs which means that these photoanode samples are very far from an ideal solar cell. This is visually apparent in the shape of the curves in **Figure 6** where the curves appear to be closer to linear than to the typical elbow shape of solar cells. The high series resistance values are likely one of the main contributors to these very low fill factor values. However, it is difficult to pinpoint what is the source of these high R_s values and will be a point of further work on this project.

Looking at the relationship between sensitization time and power, there is some correlation between the amount of time a sample is sensitized for and the amount of power it can output. It is expected that as a sample is sensitized for a longer period that it would output higher power to a certain point where overcrowding from dye molecules could possibly lead to a reduction in power output. This data does not show a sign of over sensitization, but it is inconclusive due to the low number of data points and unclear overall trend in this relationship.

To understand why there were issues with photoanode performance, SEM imaging was done to discover whether surface structure was a main issue in the photogeneration limits. The SEM imaging shown in **Figure 7** demonstrates the distinct changes in surface topology due to the annealing process. The image of the post-annealing sample demonstrates that there is a very high surface area, as expected, and an interconnected, mesoporous structure of TiO_2 nanoparticles. This means that this is undoubtably a very high surface area for reactions to take place, but it does not guarantee the conductivity of the TiO_2 film itself. Future work using ellipsometry can be done to determine the thickness of this thin film and its electrical conductivity, ideally allowing for the identification of the property limiting the performance of the photoanodes.

Conclusions

The minimum project goal of developing a working procedure for producing light-active photoanodes has been achieved as demonstrated through results from polarization tests under the illumination of a solar lamp. As shown in the results, the generation of the photoanodes described here are very low, around an order of magnitude lower than desired. However, this does serve as a proof of concept for future work to be conducted involving the increased optimization of the production process to output higher efficiency photoanodes.

The optimization process of the photoanodes will involve a detailed analysis into the individual parameters that are expected to impact the performance of these cells. Further iteration on the deposition process of the TiO_2 is necessary to create more consistent thin films as well as a deeper characterization of said thin films through testing such as ellipsometry, X-ray diffraction, and continued morphological analysis through SEM. Potential avenues for increasing the uniformity of the TiO_2 are screen printing, chemical vapor deposition, sputter coating, each of which can produce specific layer thicknesses but are all most costly than doctor blading. As a proof of concept these methods may prove to be more effective when compared to doctor blading.

Once a satisfactory level of photoanode performance has been achieved, testing in a full flow battery cell will be conducted to understand the effects of photoanode charging on a fully cycling flow cell. Eventually, testing with multiple types of electrolytes will be done to investigate performance utilizing aqueous organic electrolytes that other members of the Kwabi Lab work with. Though not originally in the plan for this project, these photoanodes are also going to serve

as part of a project involving photo-catalytically driven CO_2 capture. The baseline laid out in this paper will be used to drive further research in the usage of DSCs for photo-electrochemical work.

Acknowledgments

References

[1]   A. Gurung, Q. Q. Qiao, Joule 2018

[2]   Li, W., Kerr, E., Goulet, M.-A., Fu, H.-C., Zhao, Y., Yang, Y., Veyssal, A., He, J.-H., Gordon, R. G., Aziz, M. J., Jin, S., A Long Lifetime Aqueous Organic Solar Flow Battery. *Adv. Energy Mater.* 2019, 9, 1900918.

[3]   Li, W., & Jin, S. (2020). Design Principles and Developments of Integrated Solar Flow Batteries. *Accounts of Chemical Research, 53*(11), 2611-2621. doi:10.1021/acs.accounts.0c00373

[4]   Noak, J. (2020). Redox flow batteries for renewable energy storage. Energy Storage News. https://www.energy-storage.news/blogs/redox-flow-batteries-for-renewable-energy-storage

[5]   United States Department of Energy. (2013). Grid Energy Storage. https://www.energy.gov/sites/prod/files/2014/09/f18/Grid%20Energy%20Storage%20December%202013.pdf

[6]   Sahu, O. P., & Yimer, S. (2015). Dye-Sensitized Solar Cells by Fruits. International Journal of Green Energy, 12(4), 409–416. https://doi.org/10.1080/15435075.2013.841166

[7]   Li, W., & Jin, S. (2020). Design Principles and Developments of Integrated Solar Flow Batteries. Accounts of Chemical Research, 53(11), 2611–2621. https://doi.org/10.1021/acs.accounts.0c00373

[8]   Yu, M., Mcculloch, W. D., Beauchamp, D. R., Huang, Z., Ren, X., & Wu, Y. (2015). Aqueous Lithium–Iodine Solar Flow Battery for the Simultaneous Conversion and Storage of Solar Energy. *Journal of the American Chemical Society*, *137*(26), 8332–8335. doi: 10.1021/jacs.5b03626

[9]   Gamry Instruments. (2021). Dye Sensitized Solar Cells-Dye Solar Cells-DSSC-DSC. https://www.gamry.com/application-notes/physechem/dssc-dye-sensitized-solar-cells/